Discovery of Potent, Selective, Orally Active, Nonpeptide Inhibitors of Human Mast Cell Chymase

Michael N. Greco,*,† Michael J. Hawkins,†
Eugene T. Powell,† Harold R. Almond, Jr.,†
Lawrence de Garavilla,† Jeffrey Hall,† Lisa K. Minor,†
Yuanping Wang,† Thomas W. Corcoran,† Enrico Di Cera,‡
Angelene M. Cantwell,‡,§ Savvas N. Savvides,‡,||
Bruce P. Damiano,† and Bruce E. Maryanoff*,†

Research and Early Development, Johnson & Johnson Pharmaceutical Research and Development, Spring House, Pennsylvania 19477-0776, and Department of Biochemistry and Molecular Biophysics, Washington University, School of Medicine, St. Louis, Missouri 63110

Received January 16, 2007

Abstract: A series of β-carboxamido-phosphon(in)ic acids (**2**) was identified as a new structural motif for obtaining potent inhibitors of human mast cell chymase. For example, 1-naphthyl derivative **5f** had an IC_{50} value of 29 nM and (*E*)-styryl derivative **6g** had an IC_{50} value of 3.5 nM. An X-ray structure for **5f**·chymase revealed key interactions within the enzyme active site. Compound **5f** was selective for inhibiting chymase versus eight serine proteases. Compound **6h** was orally bioavailable in rats (F = 39%), and orally efficacious in a hamster model of inflammation.

A variety of cell types, such as neutrophils, mast cells, monocytes, macrophages, eosinophils, and lymphocytes, can play a major role in immune-mediated inflammatory diseases.[1] However, whereas the recruitment of such cells into injured tissues is crucial to tissue repair and host defense,[2] this accumulation can also be deleterious. One source of the adverse actions is secreted proteases.[3] During inflammatory events, tissue damage[4] ensues when there is an excess of protease activity that overwhelms the levels of endogenous protease inhibitors.[5] Consequently, the administration of exogenous inhibitors could rectify this imbalance and provide a therapeutic benefit, such as in pulmonary inflammatory diseases like asthma and chronic obstructive pulmonary disease (COPD).

Because asthma and COPD are serious, unmet medical needs with an expanding incidence worldwide, we developed a keen interest in the serine proteases cathepsin G (EC 3.4.21.20; Cat G)[4,6] and chymase (EC 3.4.21.39).[6a,7] These chymotrypsin-like enzymes can degrade extracellular matrix (e.g., collagen, elastin, proteoglycans, and fibronectin), induce leukocyte migration, and promote tissue remodeling.[4,6a,7a,b] We recently described **1** (JNJ-10311795) as a potent dual inhibitor of human Cat G (K_i = 38 nM) and human chymase (K_i = 2.3 nM), and established its molecular interactions in the active site of each enzyme.[8] In investigating the biological properties of **1**, we have observed notable activity in several animal models of inflammation.[8,9] To gain a better understanding of the pharmacology, especially in terms of its component actions, we set out to identify and study selective inhibitors of Cat G and chymase. We now report on the discovery of a novel series of nonpeptide chymase inhibitors possessing a β-carboxamido-phosphon(in)ic acid motif (**2**). This chemical series has yielded potent, selective inhibitors that exhibit useful oral bioavailability and promising anti-inflammatory pharmacology.

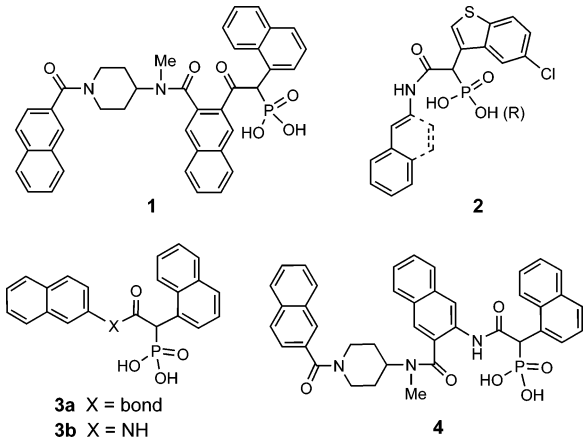

The original lead compound that led us to **1** was β-ketophosphonic acid **3a**, which was identified via high-throughput screening for inhibitors of human Cat G.[10] In exploring related structures as potential Cat G inhibitors, we prepared aza-homologue **3b**.[11] This compound was devoid of Cat G inhibition (0% inhibition at 100 μM), but had moderate potency against human chymase (IC_{50} = 190 nM).[12] Because there is a close sequence homology (>50%) between Cat G and chymase, and close structural homology between their active sites (~80%), **3b** was modeled into the chymase active site in the mode observed for **3a**·Cat G.[10] Thus, the 1-naphthyl and 2-naphthyl groups were oriented in the S2 and S1 pockets, respectively (Figure S1, Supporting Information). The vacant, hydrophobic S3/S4 region was seen as having potential for additional binding interactions via attachment of appropriate substituents to the 3-position of the 2-naphthyl group, as exemplified in **4**.[10] While this approach parallels the one that we used to progress from **3a** to **1**, with a 100-fold potency enhancement,[8] various attempts to effect this outcome with **3b** met with disappointment. For example, the chymase IC_{50} value for **4** was >10 μM. Faced with this outcome, we decided to systematically investigate structural modifications of molecule **3b**.

The 1-naphthyl ring, thought to occupy the S2 subsite of chymase, was replaced by different bicyclic heterocycles. We synthesized the target compounds by the route outlined in Scheme 1, which is exemplified for **5e** (Table 1). Triethylphosphite and 3-(bromomethyl)benzothiophene were heated at reflux to furnish diethyl (3-benzothienyl)methylphosphonate (57% yield),[13] which was deprotonated in THF with butyllithium (2.6 M in hexane), reacted with 2-naphthylisocyanate, and de-esterified with bromotrimethylsilane in pyridine to give **5e** (11% yield).

Considering the set of phosphonic acid compounds, **3b** and **5a**−**g**, potency for inhibition of human chymase varied over a 200-fold range (Table 1). Relative to the initial 1-naphthyl derivative, **3b**, the 3-benzofuranyl (**5a**) and 3-indolyl (**5b**) analogues were less potent, the 3-benzothienyl (**5e**) and 3-(1-methylindolyl) (**5c**) analogues were marginally more potent, but

* To whom correspondence should be addressed. Tel.: 215-628-5614 (M.N.G.); 215-628-5530 (B.E.M.). Fax: 215-628-4985 (M.N.G. and B.E.M.). E-mail: mgreco@prdus.jnj.com (M.N.G.); bmaryano@prdus.jnj.com (B.E.M.).

† Johnson & Johnson Pharmaceutical Research and Development.

‡ Washington University, School of Medicine.

§ Present address: Department of Microbiology and Immunology, University of Texas Health Science Center, San Antonio, TX 78229.

|| Present address: Laboratory for Protein Biochemistry and Protein Engineering, Ghent University, 9000 Ghent, Belgium.

10.1021/jm0700619 CCC: $37.00
Published on Web 03/16/2007

Scheme 1. Synthesis of **5e**

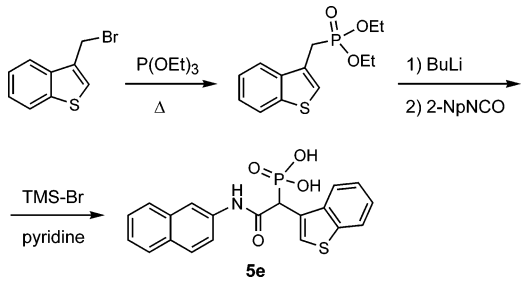

5e

Table 1. Structures and Chymase Inhibiton Data for *N*-(2-Naphthyl)carboxamido Derivatives

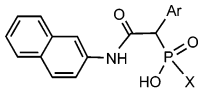

5

cmpd[a]	Ar	X	IC_{50}[b] (nM)
3b	1-naphthyl	OH	190 (1)
5a	3-benzofuranyl	OH	2500 ± 560 (4)
5b	3-indolyl	OH	920 ± 530 (2)
5c	3-(1-methylindolyl)	OH	90 ± 28 (4)
5d	3-(1-Me-5-chloroindolyl)	OH	13 ± 7 (2)
5e	3-benzothienyl	OH	120 ± 30 (4)
5f	3-(5-chlorobenzothienyl)	OH	29 ± 9 (2)[c]
5g	1-benzotriazolyl	OH	NA
5h	3-(1-Me-5-chloroindolyl)	Me	10 ± 0 (2)
5i	3-(5-chlorobenzothienyl)	Me	80 ± 4 (2)
5j	1-naphthyl	Me	210 ± 70 (2)
5k	3-(5-chlorobenzothienyl)	Et	160 ± 4 (2)
5l	3-(5-chlorobenzothienyl)	Ph	2100 ± 200 (2)
5m	3-(5-chlorobenzothienyl)	$Ph(CH_2)_2$	240 ± 10 (2)
1[d]			4.5

[a] New compounds were purified, isolated as phosphonic or phosphinic acids, and characterized by ES-MS and ^{1}H NMR (Supporting Information). All new compounds are racemates. The stereogenic center is labile according to ^{1}H NMR H−D exchange experiments with certain derivatives. [b] Inhibition of human chymase as gauged by mean IC_{50} values; number of experiments, *N*, is given in parentheses, with error limits for $N \geq 2$. NA, <50% inhibition at 10 μM. [c] K_i = 36 nM (K_i for Cat G = 9500 nM). [d] Reported in ref 8.

the 3-(5-chlorobenzothienyl) (**5f**) and 3-(1-methyl-5-chloroindolyl) (**5d**) analogues were notably more potent (IC_{50} values of 29 and 13 nM, respectively). Thus, a 5-chloro group enhanced potency by a factor of 4−5 over a 5-position hydrogen. Nitrogen-linked benzotriazole **5g** was essentially devoid of inhibitory activity.

An X-ray crystallographic study on the 1:1 complex of **5f** and human chymase was very revealing (Figures 1 and 2).[14] Notably, the 5-chlorobenzothiophene group *occupies the S1 pocket* and the 2-naphthyl group *occupies the S2 domain*, which is *opposite* from what we had anticipated and explains why **4** is such a poor chymase inhibitor. The various close contacts that lead to important ligand−enzyme interactions are depicted in Figure 2. The phosphonate moiety is involved in a complex hydrogen-bonding network: one oxygen atom is in the oxyanion hole, interacting with Gly-193 Nα and Ser-195 Oγ; a second oxygen interacts with Ser-195 Oγ and His-57 Nϵ; and a third oxygen interacts with Lys-192 Nϵ. Additionally, the amide NH of the ligand forms a key hydrogen bond with the Ser-214 C═O and the amide carbonyl interacts with Lys-192 Nϵ. With this crystallographic information, we could now modify the structure of the ligand more rationally, to improve druggability (e.g., absorption/ distribution/metabolism/excretion properties) while retaining potency. In this regard, **5f** exhibited low oral bioavailability in rats (F = 3%; oral $t_{1/2}$ = 1.8 h).

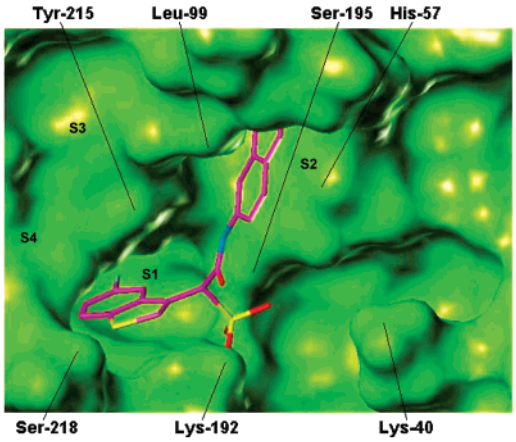

Figure 1. Crystal structure of the **5f**·chymase complex. View of the **5f** (stick model) within the chymase active site (Connelly surface: green), with labeling of key amino acids.

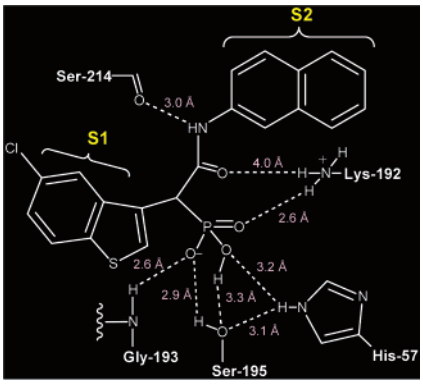

Figure 2. Depiction of the principal interactions between **5f** and the amino acid residues of chymase.

One approach that we pursued was replacement of a single P−OH with a P−C group, thereby generating phosphinate analogues (Table 1, **5h**−**m**). Although this change sacrifices a key P−O H-bond interaction (Figure 2), the crystal structure indicated that a small alkyl would be tolerated sterically. Interestingly, the phosphinates with X = Me, **5h**−**j**, have essentially the same potency as their phosphonate counterparts, **5d**, **5f**, and **3b**, respectively. However, the *P*-Et (**5k**) and *P*-$(CH_2)_2$Ph (**5m**) analogues have reduced potency by a factor of 2−3, and the *P*-Ph analogue (**5l**) has reduced potency by a factor of 25.

Our optimization effort was extended to a series of *N*-[(*E*)-styryl] derivatives, exemplified by **6a**−**k** (Table 2). A representative synthesis is outlined in Scheme 2. Diethyl methylphosphonite and 3-(bromomethyl)-5-chlorobenzothiophene were heated at reflux to give the intermediate phosphinate (80% yield),[13] which was deprotonated in THF with butyllithium (2.6 M in hexane), reacted with 2-[(*E*)-3-chlorostyryl]isocyanate, and de-esterified with bromotrimethylsilane to give **6g** (74% yield). The requisite isocyanate was obtained by reacting (*E*)-3-chlorocinnamic acid and diphenyl phosphoryl azide, followed by thermal rearrangement of the intermediate acyl azide (benzene, reflux, 15 h).

Replacement of the 2-naphthyl group in **5** with the (*E*)-styryl group in **6** worked out quite well, as the naphthyl/styryl pairs have nearly the same IC_{50} values (Table 2). By way of illustration, the corresponding naphthyl/styryl phosphonate pairs **5f**/**6a** and **5d**/**6e** have IC_{50} values of 29/60 and 13/16 nM; the corresponding phosphinate pairs **5i**/**6i** and **5h**/**6j** have IC_{50} values of 80/58 and 10/21 nM.[15] In analogy to series **5**, *P*-ethyl

Table 2. Structures and Chymase Inhibiton Data for *N*-(2-Styryl)carboxamido and Related Derivatives

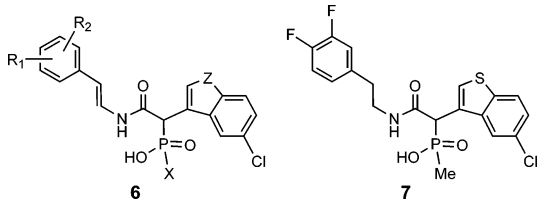

cmpd[a]	X	Z	R_1	R_2	IC_{50}[b] (nM)
6a	OH	S	H	H	60 ± 20 (3)
6b	OH	S	H	4-F	66 ± 10 (6)
6c	OH	S	3-F	4-F	11 ± 0 (2)
6d	OH	S	H	4-OMe	280 ± 110 (2)
6e	OH	NMe	H	4-F	16 ± 5 (2)
6f	Me	S	H	H	50 ± 10 (2)
6g	Me	S	3-Cl	H	3.5 ± 1 (2)
6h	Me	S	3-Cl	5-F	17 ± 2 (4)
6i	Me	S	3-F	4-F	58 ± 12 (7)
6j	Me	NMe	3-F	4-F	21 ± 4 (2)
6k	Et	S	3-F	4-F	165 ± 12 (2)
7[c]					10 400 ± 100 (2)

[a] See footnote a in Table 1. [b] Mean IC_{50} values; number of experiments, *N*, is given in parentheses; error limits are given for $N \geq 2$. [c] Analogue of **6i** with the C−C double bond saturated.

Scheme 2. Synthesis of **6g**

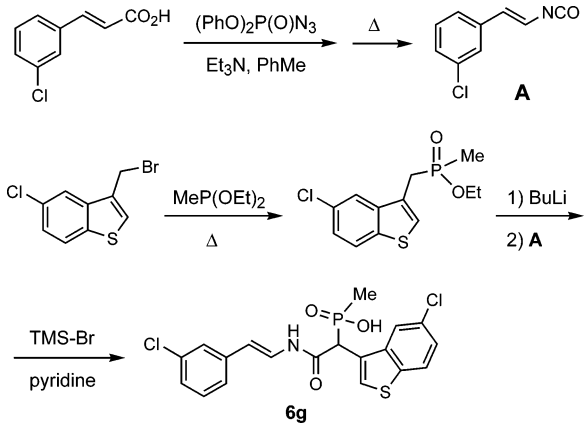

phosphinate **6k** had a moderate reduction in potency (IC_{50} = 165 nM) relative to *P*-methyl phosphinate **6i** (IC_{50} = 58 nM). We were able to achieve single-digit nanomolar potency with a phosphinate moiety, as shown for 3-chloro analogue **6g** (IC_{50} = 3.5 nM). It is noteworthy that such high potency is possible while using only two P−O groups. In this subclass, going from a phosphonate to a phosphinate may leave the potency unchanged (cf. **3b** and **5j**) or cause a moderate 5-fold loss in potency (cf. **6c** and **6i**). Remarkably, the carbon−carbon double bond was very critical for potent chymase inhibition: whereas **6i** has an IC_{50} of 58 nM, saturated analogue **7** has an IC_{50} of 10 400 nM (180-fold less potent). Thus, a certain geometry and conformational constraint is required for optimal interactions in the S2 region.

Chymase inhibitor **5f** (IC_{50} = 29 nM) was examined for enzyme selectivity with a panel of eight serine proteases. It displayed high selectivity versus Cat G (IC_{50} = 12 μM), chymotrypsin (NA), trypsin (IC_{50} = 12 μM), β-tryptase (NA), α-thrombin (NA), factor Xa (NA), factor VIIa, and leukocyte elastase (NA).[16] The enzyme kinetics for chymase inhibition showed Michaelis−Menten competitive behavior. In the case of **5f**, a K_i value of 36 nM was measured. Comparing K_i values (Table 1, footnote c), the selectivity of **5f** for chymase over Cat G was about 260-fold. We tested the chymase inhibition mechanism with **6c** and confirmed the absence of slow-tight binding.[17]

Favorable rat pharmacokinetics data were obtained for 3-chloro-5-fluoro analogue **6h** (IC_{50} = 17 nM; K_i = 11 nM): F = 39%, oral $t_{1/2}$ = 4.5 h, C_{max} = 6 μM.[18] Given this good oral bioavailability, **6h** was administered orally in a hamster model of inflammation.[19] The test compound was dosed at 30 mg/kg, p.o., for 3 days and then at 2 h prior to carrageenan administration on day 4. In the **6h**-treated hamsters, the increase in paw volume caused by carrageenan, which was marked at 4 h post challenge, was inhibited by about 50% (Figure S2). For comparison, administration of the anti-inflammatory steroid dexamethasone at 10 mg/kg, i.m., 2 h prior to carrageenan challenge, completely blocked the increase in paw volume (Figure S2).

By manipulating our original β-ketophosphonate inhibitors of human Cat G and chymase,[8,10] with the aid of structure-based design, we identified a series of β-carboxamido-phosphon(in)ic acids, **2**, which contain potent, selective inhibitors of human mast cell chymase. For example, 2-naphthyl derivative **5f** had a chymase K_i value of 36 nM and a Cat G K_i value of 9500 nM (ca. 260-fold selectivity), and (*E*)-styryl derivative **6g** had single-digit nanomolar potency (chymase IC_{50} = 3.5 nM). X-ray crystallography on **5f**·chymase revealed the key interactions within the enzyme active site. Given the complex hydrogen-bonding network around the phosphonate group, it was surprising that we could eliminate one of the oxygen atoms and still achieve excellent potency. This replacement and the paring down of the 2-naphthyl group to an (*E*)-styryl group were crucial for obtaining favorable rat pharmacokinetics. Compound **6h** was not only orally bioavailable in rats (F = 39%), but was also effective in a hamster model of inflammation on oral administration. Although useful cardiovascular pharmacology has been associated with chymase inhibitors from studies in animal models,[20] our observation constitutes the first report of marked anti-inflammatory activity for a chymase inhibitor.

Acknowledgment. We thank our spectroscopy group for analytical characterization data.

Supporting Information Available: Details for the synthetic procedures, product characterization, biological assay procedures, and X-ray crystallography. Figures S1 and S2. This material is available free of charge via the Internet at http://pubs.acs.org.

References

(1) (a) Holgate, S. T. The role of mast cells and basophils in inflammation. *Clin. Exp. Allergy* **2000**, *1*, 28−32. (b) Pearlman, D. S. Pathophysiology of the inflammatory response. *J. Allergy Clin. Immunol.* **1999**, *104*, S132−S137. (c) Borish, L.; Joseph, B. Z. Inflammation and the allergic response. *Med. Clin. North Am.* **1992**, *76*, 765−787. (d) Rhee, J. S.; Santoso, S.; Herrmann, M.; Bierhaus, A.; Kanse, S. M.; May, A. E.; Nawroth, P. P.; Colman, R. W.; Preissner, K. T.; Chavakis, T. New aspects of integrin-mediated leukocyte adhesion in inflammation: regulation by haemostatic factors and bacterial products. *Curr. Mol. Med.* **2003**, *3*, 387−392.

(2) (a) Chertov, O.; Yang, D.; Howard, O. M.; Oppenheim, J. J. Leukocyte granule proteins mobilize innate host defenses and adaptive immune responses. *Immunol. Rev.* **2000**, *177*, 68−78. (b) Tani, K.; Ogushi, F.; Shimizu, T.; Sone, S. Protease-induced leukocyte chemotaxis and activation: roles in host defense and inflammation. *J. Med. Invest.* **2001**, *48*, 133−141.

(3) (a) Lehr, H. A.; Arfors, K. E. Mechanisms of tissue damage by leukocytes. *Curr. Opin. Hematol.* **1994**, *1*, 92−99. (b) Shapiro, S. D. Proteinases in chronic obstructive pulmonary disease. *Biochem. Soc. Trans.* **2002**, *30*, 98−102.

(4) (a) Caughey, G. H. Serine proteinases of mast cell and leukocyte granules. A league of their own. *Am. J. Respir. Crit. Care Med.* **1994**, *150*, S138−S142. (b) Bank, U.; Ansorge, S. More than destructive: neutrophil-derived serine proteases in cytokine bioactivity control. *J. Leukocyte Biol.* **2001**, *69*, 197−206. (c) Caughey, G. H.; Nadel, J. A. Proteases. *Asthma*; Barnes, P. J., Ed.; Lippincott Williams & Wilkins: Philadelphia, PA, 1997; Vol. 1, pp 609−625.

(5) (a) Stockley, R. A. Neutrophils and protease/antiprotease imbalance. *Am. J. Respir. Crit. Care Med.* **1999**, *160*, S49−S52. (b) Simon, S. R. Oxidants, metalloproteases and serine proteases in inflammation. *Agents Actions Suppl.* **1993**, *42*, 27−37.

(6) (a) Owen, C. A.; Campbell, E. J. The cell biology of leukocyte-mediated proteolysis. *J. Leukocyte Biol.* **1999**, *65*, 137−150 [see comment]. (b) Owen, C. A.; Campbell, E. J. Neutrophil proteinases and matrix degradation. The cell biology of pericellular proteolysis. *Semin. Cell Biol.* **1995**, *6*, 367−376. (c) Hanson, R. D.; Connolly, N. L.; Burnett, D.; Campbell, E. J.; Senior, R. M.; Ley, T. J. Developmental regulation of the human cathepsin G gene in myelomonocytic cells. *J. Biol. Chem.* **1990**, *265*, 1524−1530.

(7) (a) Hart, P. H. Regulation of the inflammatory response in asthma by mast cell products. *Immunol. Cell Biol.* **2001**, *79*, 149−153. (b) Caughey, G. H. Mast cell chymases and tryptases: phylogeny, family relations, and biogenesis. *Mast Cell Proteases in Immunology and Biology*; Marcel-Decker: New York, 1995; pp 305−329. (c) Miller, H. R.; Pemberton, A. D. Tissue-specific expression of mast cell granule serine proteinases and their role in inflammation in the lung and gut. *Immunology* **2002**, *105*, 375−390. (d) Schechter, N. M.; Pereira, P. J. B.; Strobl, S. Structure and function of human chymase. *Mast Cells and Basophils*; Marone, G., Lichtenstein, L. M., Galli, S. J., Eds.; Academic Press: London, U.K., 2000; pp 275−290. (e) Compton, S. J.; Cairns, J. A.; Holgate, S. T.; Walls, A. F. The role of mast cell tryptase in regulating endothelial cell proliferation, cytokine release, and adhesion molecule expression: tryptase induces expression of mRNA for IL-1β and IL-8 and stimulates the selective release of IL-8 from human umbilical vein endothelial cells. *J. Immunol.* **1998**, *161*, 1939−1946.

(8) de Garavilla, L.; Greco, M. N.; Sukumar, N.; Chen, Z.-W.; Pineda, A. O.; Mathews, F. S.; Di Cera, E.; Giardino, E. C.; Wells, G. I.; Haertlein, B. J.; Kauffman, J. A.; Corcoran, T. W.; Derian, C. K.; Eckardt, A. J.; Damiano, B. P.; Andrade-Gordon, P.; Maryanoff, B. E. A novel, potent dual inhibitor of the leukocyte proteases cathepsin G and chymase: molecular mechanisms and anti-inflammatory activity in vivo. *J. Biol. Chem.* **2005**, *280*, 18001−18007.

(9) de Garavilla, L.; Wells, G. I. Unpublished results.

(10) Greco, M. N.; Hawkins, M. J.; Powell, E. T.; Almond, H. R., Jr.; Corcoran, T. W.; de Garavilla, L.; Kauffman, J. A.; Recacha, R.; Chattopadhyay, D.; Andrade-Gordon, P.; Maryanoff, B. E. Nonpeptide inhibitors of cathepsin G: optimization of a novel beta-ketophosphonic acid lead by structure-based drug design. *J. Am. Chem. Soc.* **2002**, *124*, 3810−3811.

(11) Greco, M. N.; Hawkins, M. J.; Powell, E. T. Unpublished results.

(12) Compound **3a** also inhibited chymase with moderate potency (IC_{50} = 400 nM).

(13) Standard Michaelis−Arbusov reaction conditions (see Supporting Information).

(14) X-ray crystallographic study of **5f**·chymase: The **5f**·chymase complex crystallized in a tetragonal crystal form (space group $P4_3$ with $a = b = 73.94$ Å, $c = 49.45$ Å, and one molecule in the asymmetric unit), which diffracted X-rays to 2.6 Å resolution. The structure was determined by molecular replacement by using the chymase/succinyl-Ala-Ala-Pro-Phe-chloromethylketone complex (PDB entry 1PJP). Inhibitor **5f** could be unambiguously modeled in $2F_0 - F_c$ and $F_0 - F_c$ electron-density maps, and the structure was refined (2.6 Å resolution; R, $R_{free} = 0.229, 0.274$). Atomic coordinates and structure factors for the **5f**·chymase complex have been deposited with the Protein Data Bank (www.rcsb.org; accession code 2HVX). Additional details for the crystallographic study are provided in Supporting Information.

(15) Note: A chloro substituent on the bicyclic heterocycle in compounds **6** is important for potency. For example, the des-chloro analogue of **6c** ($IC_{50} = 130 \pm 40$ nM, $N = 4$) is 13-fold less potent than **6c**.

(16) All of the enzymology work involved human enzymes. Details for chymase and Cat G are contained in ref 8; other details are included in the Supporting Information. NA stands for <50% at 100 μM.

(17) Determined by comparing the enzyme kinetics with and without preincubation (see Supporting Information).

(18) Details of the rat PK study are included in Supporting Information.

(19) The pro-inflammatory agent carrageenan induces an acute cutaneous response, mediated primarily by mast cells. In this hamster paw edema model, carrageenan was injected into the intraplantar space of the hind paw, causing a 40−50% increase in paw volume. Anti-inflammatory activity was gauged by the reduction in paw volume. Further details on the hamster model are included in the Supporting Information.

(20) (a) Bacani, C.; Frishman, W. H. Chymase: a new pharmacological target in cardiovascular disease. *Cardiol. Rev.* **2006**, *14*, 187−193. (b) Leckie, B. J. Targeting the renin-angiotensin system: What's new? *Curr. Med. Chem.: Cardiovasc. Hematol. Agents* **2005**, *3*, 23−32. (c) Fukami, H.; Okunishi, H.; Miyazaki, M. Chymase: Its pathophysiological roles and inhibitors. *Curr. Pharm. Des.* **1998**, *4*, 439−453. (d) Akahoshi, F. Chymase inhibitors and their therapeutic potential. *Drugs Future* **2002**, *27*, 765−770.

JM0700619